Electronic Supplementary Information for: Non-covalent adsorption of Amino Acid Analogues on Noble-metal Nanoparticles: Influence of Edges and Vertices

Z. E. Hughes[a] **and Tiffany R. Walsh**[*a]

[a] Institute for Frontier Materials, Deakin University, Geelong, 3216, VIC, Australia; Email: tiffany.walsh@deakin.edu.au

Contents

Table S8: Adsorption energies of adsorbates on the Pt_{147} $\{111\}$ facet and the Pt(111) infinite planar surface. Experimental data, where available, are also presented.

Table S9: Adsorption energies for methane and water adsorbed at different sites on the Au_{147} NP calculated using a range of plane wave cutoffs.

References

Table S1: Out-of-plane displacements (Å) for centre-of-facet atom(s) calculated for Au_{147} using different functionals.

Functional	Buckling / Å	
	{111}	{100}
PBE	0.44	0.32
revPBE	0.45	0.32
revPBE-vdW-DF	0.45	0.38
PBEsol	0.37	0.29

Table S2: Inter-plane spacings of Au_{147} in the <111> and <100> directions calculated using the revPBE-vdW-DF functional. The central layer is labelled as 0.

Layer	Distance / Å	
	<111>	<100>
d_{01}	2.4671	2.0797
d_{12}	2.3510	2.0940
d_{23}	2.2114	2.0847

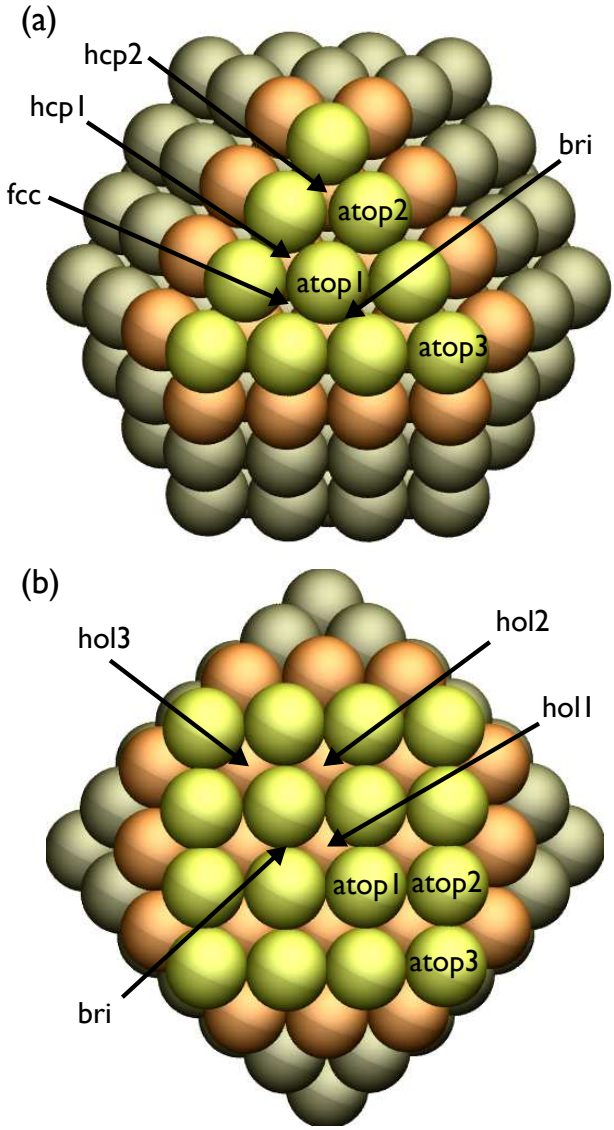

Figure S1: Different sites of the NM_{147} cuboctahedral NPs on the (a) {111} facet, and (b) {100} facet.

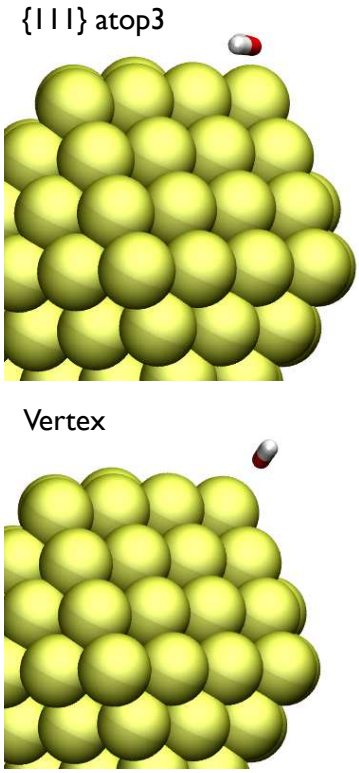

Figure S2: Example of the difference between the adsorption configuration of the {111}-atop3 site and vertex site of the NM_{147} cuboctahedral NP.

Table S3: Distance between the absorbates and NMNPs, d_{sep}, for the optimal geometries at the facets, edge and vertex sites. For hetroatomic adsorbates the distance corresponds to that between the hetroatom and the nearest metal atom. For the hydrocarbons the distance given is defined as that between the centre of mass of the carbon atoms and the surface, for the facets, or the closest one/two metal atoms for the vertex/edge.

Adsorbate	Metal	d_{sep} / Å			
		{111}	{100}	Edge	Vertex
Methane	Au	3.79	3.72	3.56	3.58
	Pt	3.83	3.77	3.67	3.48
Ethane	Au	3.95	3.82	3.77	3.63
	Pd	3.87	3.89	3.79	3.55
Benzene	Au	3.55	3.40	3.13	3.03
	Pd	3.47	2.11	2.32	2.69
Water	Au	3.02	2.86	2.85	2.63
	Pt	2.77	2.63	2.52	2.38
Methanol	Au	2.87	2.79	2.73	2.53
	Pt	2.59	2.48	2.41	2.31
Methanamide	Au	2.75	2.62	2.58	2.40
	Pt	2.41	2.30	2.27	2.41
Methanamine	Au	2.45	2.37	2.37	2.31
	Pt	2.24	2.21	2.22	2.19
Imidazole	Au	2.36	2.31	2.29	2.23
	Pt	2.14	2.17	2.14	2.14
Dimethyl	Au	2.66	2.60	2.54	2.49
Sulphide	Pt	2.35	2.39	2.34	2.34

Table S4: Adsorption energies, E_{ads}, of water on the Au(111) and Au(100) infinite planar surfaces and the $\{111\}$ and $\{100\}$ facets of Au_{147}.

Facet	Site	E_{ads} / kJ mol^{-1}	
		Au_{147}	Planar surface
(111)	atop1	-15.6	-18.3[a]
	atop2	-17.0	
	atop3	**-20.5**	
	bri	-14.2	-16.3
	fcc	-12.6	-16.5
	hcp1	-12.7	-16.4
	hcp2	-12.8	
(100)	atop1	-19.0	-20.8[a]
	atop2	-18.1	
	atop3	**-19.4**	
	bri	-15.2	-17.7[a]
	hol1	-15.9	-15.1[a]
Edge	atop	-17.7	
Vertex	atop	**-20.8**	

[a] Ref[1]

Table S5: Adsorption energies, E_{ads}, of methane at different sites on Au_{147}. Adsorption energies at corresponding sites on the infinite surface are given in parentheses.

Facet	Site	E_{ads} / kJ mol^{-1}
(111)	fcc	-11.9 (-16.5[a])
(111)	hcp1	-11.7
(111)	hcp2	-10.5
(100)	hol1	-13.9 (-16.3[a])
(100)	hol2	-13.2
(100)	hol3	-12.4
Edge	atop	-10.1
Vertex	atop	-7.7

[a] Ref[1]

Table S6: Adsorption energies, E_{ads}, of benzene at different sites on Au_{147}. Where applicable the adsorption energy at each corresponding site on the infinite planar Au(111) and Au(100) surfaces is given in parentheses.

Facet	Site	E_{ads} / kJ mol^{-1}
{111}	atop1:0°[c]	-36.5 (-54.0[a])
{111}	atop1:30°[d]	-36.2 (-53.5[a])
{111}	fcc:0°[c]	-39.2 (-56.3[a])
{111}	fcc:30°[d]	-39.2 (-56.5[a])
{100}	hol1	-48.1 (-57.9[b])
Edge	atop	-33.4
Edge	bri	-40.8
Vertex	atop	-38.7
Vertex	perp[d]	-11.3

[a] Ref[2]; [b] Ref[1]; [c] 0°: C-C bonds aligned along direction of atoms; [d] 30°: C-C bonds aligned along direction of hollow sites; [e] plane of ring parallel of vertex atom.

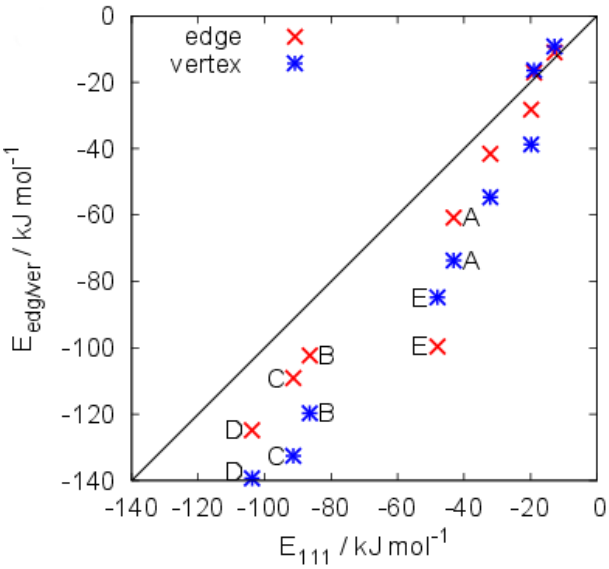

Figure S3: Comparison of adsorption energies on the {111} facet against the edge and vertex sites of the Pt_{147} cuboctahedral NP. The labels for the different molecules are: A-methanamide, B-methanamine, C-imidazole and D-dimethyl sulphide, E-benzene.

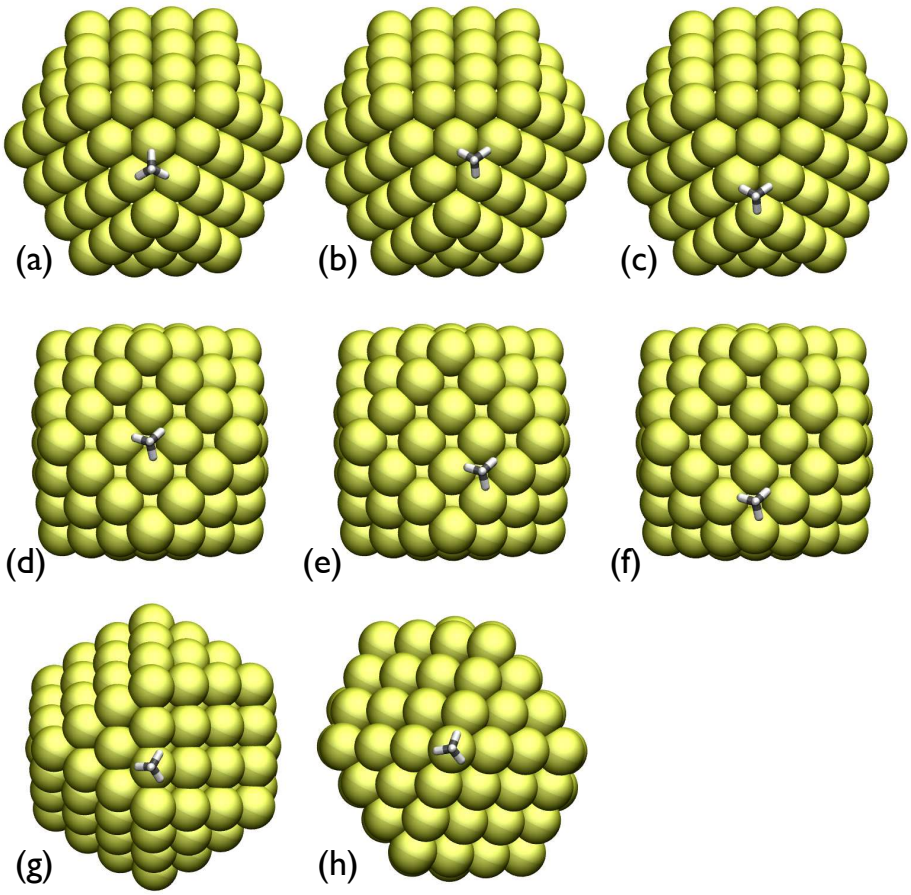

Figure S4: Optimised geometries of methane adsorbed on Au_{147}: (a) {111} facet - fcc, (b) {111} facet - hcp1, (c) {111} facet - hcp2, (d) {100} facet - hol1, (e) {100} facet - hol2, (f) {100} facet - hol3, (g) edge, and (h) vertex.

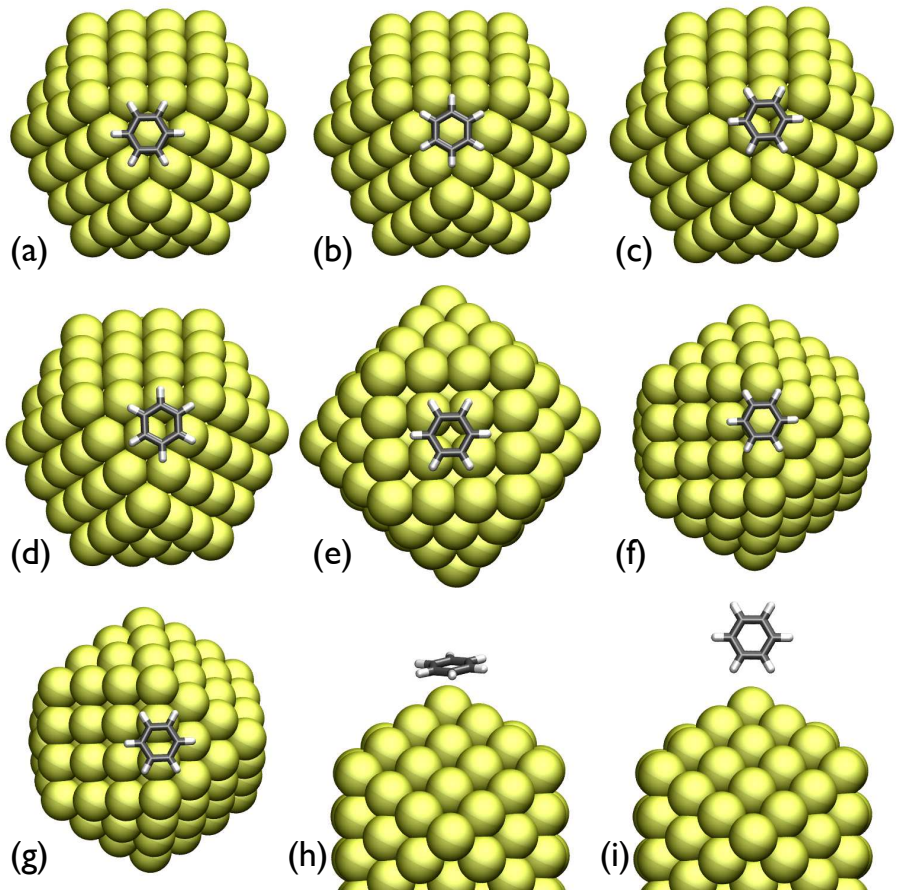

Figure S5: Optimised geometries of benzene adsorbed on Au_{147}: (a) {111} facet - atop1:0°, (b) {111} facet - atop1:30°, (c) {111} facet - fcc0°, (d) {111} facet - fcc30°, (e) {100} facet - hol1, (f) edge - atop, (g) edge - bri, (h) vertex - atop and (i) vertex - perpendicular.

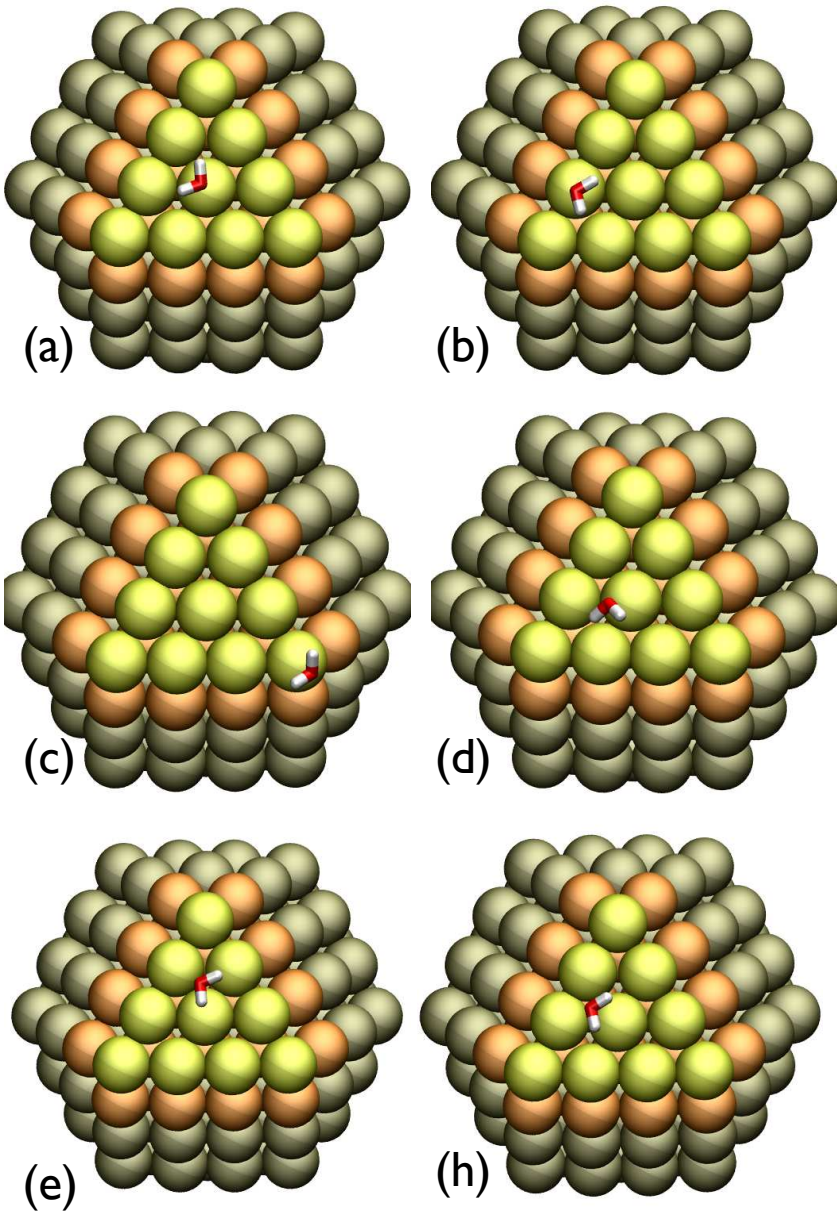

Figure S6: Optimised geometries of water adsorbed on {111} facet of Au_{147}: (a) atop1, (b) atop2, (c) atop3, (d) bri, (e) fcc, (f) hcp1.

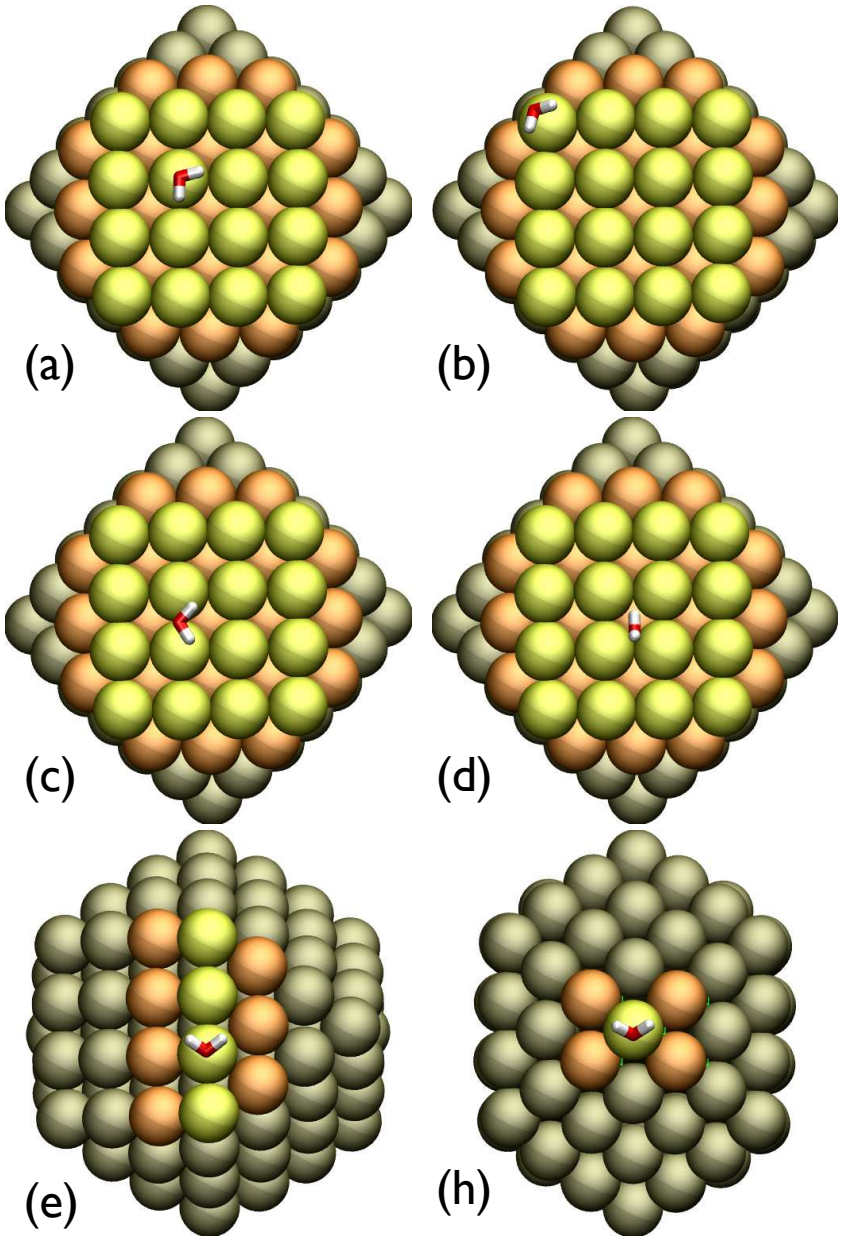

Figure S7: Optimised geometries of water adsorbed on Au_{147}: (a) {100} facet - atop1, (b) {100} facet - atop3, (c) {100} facet - bri, (d) {100} facet - hol1, (e) edge and (f) vertex.

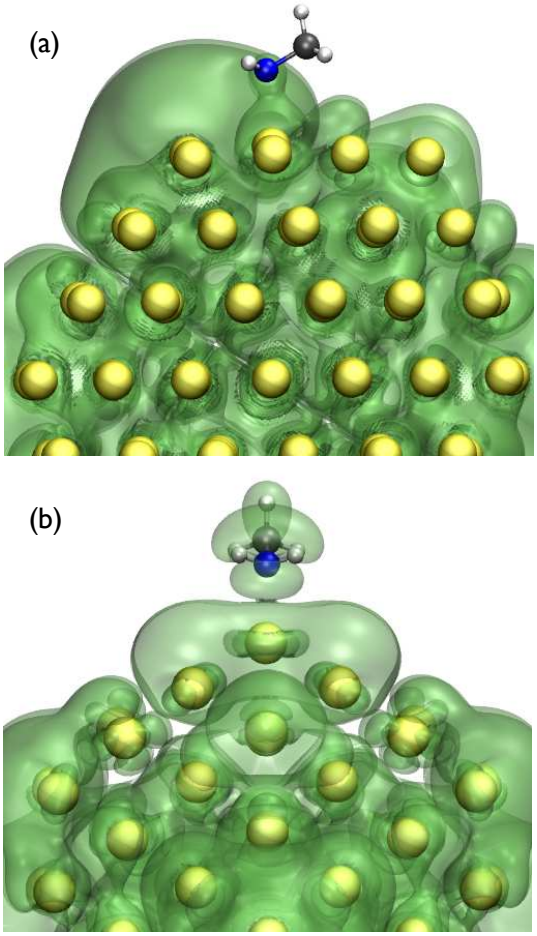

Figure S8: Isosurfaces of representative bonding orbitals for the adsorption of methanamine for (a) on the $\{111\}$ facet and (b) the vertex of Au_{147}.

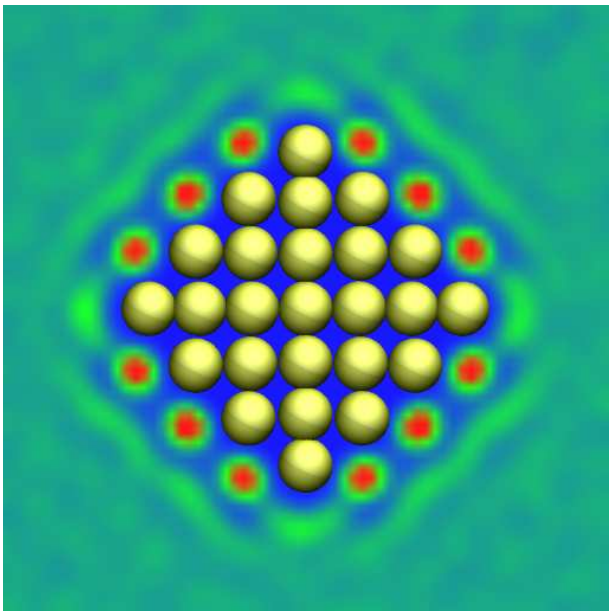

Figure S9: Interfacial water structuring averaged from molecular dynamics simulations of Au_{147} under aqueous conditions using CHARMM-METAL. A cross-section of the central region of the NP is shown. Red and blue colors indicate regions of highest and lowest density respectively.

Table S7: Energies, E_{ads}, of molecules adsorbed to the {111} and {100} facets of Au_{147}, and at corresponding sites on the infinite planar Au(111) and Au(100) surfaces. Experimental data for planar surfaces and nanoparticle surfaces are also presented for comparison; ”-” signifies that no reliable experimental data were available.

Molecule	E_{ads} / kJ mol^{-1}				
	(111)		(100)		Expt.
	Au_{147}	Planar surface	Au_{147}	Planar surface	
Methane	-11.9	-16.5[a]	-13.9	-16.3[a]	-14.5[c]
Ethane	-17.8	-24.7[a]	-20.4	-24.5[a]	-24.1[c]
Benzene	-39.2	-56.5[b]	-48.1	-57.9[a]	-57.9,[c] -61.5,[d] -62.7, [e], -28.0,[f] -48.7[g]
Water	-15.6	-18.3[a]	-19.0	-20.8[a]	-
Methanol	-25.3	-30.5[a]	-29.5	-31.7[a]	-
Methanamide	-31.3	-34.2[a]	-38.6	-34.9[a]	-
Methanamine	-53.1	-54.8[a]	-64.2	-61.3[a]	-
Imidazole	-55.7	-54.1[a]	-66.9	-67.2[a]	-
Dimethyl sulphide	-59.3	-63.9	-71.1	-69.1[a]	-

[a] Ref[1] DFT revPBE-vdW-DF functional;
[b] Ref[2] DFT revPBE-vdW-DF functional;
[c] Ref[3] Au(111) surface temperature programmed desorption;
[d] Ref[4] Au(111) surface temperature programmed desorption;
[e] Ref[5] Au(111) surface temperature programmed desorption;
[f] Ref[6] AuNP on Al_2O_3 support chromatography;
[g] Ref[7] AuNP on silica support chromatography.

Table S8: Comparison of calculated adsorption energies, E_{ads}, of molecules to both the Pt(111) planar Pt_{147} $\{111\}$ nanoparticle surfaces. Experimental data for planar surfaces are also presented for comparison; ”-” signifies that no experimental/DFT data were available.

Molecule	Surface/facet	E_{ads} / kJ mol^{-1}		
		Pt_{147} calculation	Planar surface experiment	Planar surface DFT calculation
Methane	(111)	-12.8	-15.2,[a] -16.1[b]	-
Ethane	(111)	-18.9	-28.9,[a] -36.8[b]	-
Benzene	(111)	-48.0	-123.0 to -167.0[c]	-74.3,[d] -94.6[e]
Water	(111)	-19.8	-	-23.3[f]

[a] Ref[8] Pt(111) surface temperature programmed desorption;
[b] Ref[9] Pt(111) surface temperature programmed desorption;
[c] Ref[10] Pt(111) surface single crystal adsorption calorimetry;
[d] Ref[11] Pt(111) surface DFT revPBE-vdW-DF functional;
[e] Ref[12] Pt(111) surface DFT revPBE-vdW-DF functional;
[f] Ref[13] Pt(111) surface DFT revPBE-vdW-DF functional;

Table S9: Adsorption energies, E_{ads}, for methane and water adsorbed at different sites on the Au_{147} NP calculated at a range of plane wave cutoffs.

System	Cutoff / Ry	E_{ads}/ kJ mol^{-1}			
		{111}	{100}	Edge	Vertex
Water	25	-15.6	-19.0	-17.7	-20.8
	35	-15.6	-18.9	-17.7	-20.8
	50	-15.3	-18.6	-17.5	-20.6
Methane	25	-11.9	-13.9	-10.1	-7.7
	35	-12.1	-14.0	-10.2	-7.6
	50	-12.5	-14.4	-10.6	-7.9

References

[1] L. B. Wright, P. M. Rodger, S. Corni and T. R. Walsh, *J. Chem. Theory Comput.*, 2013, **9**, 1616–1630.

[2] Z. E. Hughes, L. B. Wright and T. R. Walsh, *Langmuir*, 2013, **29**, 13217–13229.

[3] S. M. Wetterer, D. J. Lavrich, T. Cummings, S. L. Bernasek and G. Scoles, *J. Phys. Chem. B*, 1998, **102**, 9266–9275.

[4] D. Syomin, J. Kim, B. E. Koel and G. B. Ellison, *J. Phys. Chem. B*, 2001, **105**, 8387–8394.

[5] W. Liu, F. Maass, M. Willenbockel, C. Bronner, M. Schulze, S. Soubatch, F. S. Tautz, P. Tegeder and A. Tkatchenko, *Phys. Rev. Lett.*, 2015, **115**, 036104.

[6] V. V. Smirnov, S. N. Lanin and A. Y. Vasil'kov, *Russ. Chem. Bull. Int. Ed.*, 2005, **54**, 2286–2289.

[7] M. Clément and H. Ménard, *Langmuir*, 2010, **26**, 8309–8312.

[8] S. L. Tait, Z. Dohnálek, C. T. Campbell and B. D. Kay, *J. Chem. Phys.*, 2006, **125**, 234308.

[9] J. F. Weaver, A. F. Carlsson and R. J. Madix, *Surf. Sci. Rep.*, 2003, **50**, 107–199.

[10] H. Ihm, H. M. Ajo, J. M. Gottfried and P. Bera, *J. Phys. Chem. B*, 2004, **108**, 14627–14633.

[11] J. Carrasco, W. Liu, A. Michaelides and A. Tkatchenko, *J. Chem. Phys.*, 2014, **140**, 084704.

[12] H. Yildirim, T. Greber and A. Kara, *J. Phys. Chem. C*, 2013, **117**, 20572–20583.

[13] J. Carrasco, J. Klimeš and A. Michaelides, *J. Chem. Phys.*, 2013, **138**, 024708.